International Journal of Multiphase Flow 36 (2010) 755–768

Contents lists available at ScienceDirect

International Journal of Multiphase Flow

journal homepage: www.elsevier.com/locate/ijmulflow

An application of the wavelet analysis technique for the objective discrimination of two-phase flow patterns

Van Thai Nguyen [a,b], Dong Jin Euh [b], Chul-Hwa Song [a,b,*]

[a] University of Science and Technology, 113 Gwahangno, Yuseong, Daejeon 305-333, Republic of Korea
[b] Korea Atomic Energy Research Institute, Daedeok-daero 1045, Yuseong, Daejeon 305-353, Republic of Korea

ARTICLE INFO

Article history:
Received 23 December 2009
Received in revised form 28 April 2010
Accepted 30 April 2010
Available online 6 May 2010

Keywords:
Two-phase flow patterns
Void fraction
Continuous Wavelet Transform
Local wavelet energy coefficient

ABSTRACT

This paper presents an application of the wavelet analysis technique for two-phase flow pattern identification by using the void fraction signals obtained from a multi-channel Impedance Void Meter (IVM) in a vertical-upward air–water flow. A new method for the objective discrimination of the two-phase flow pattern has been developed to provide information regarding the local energy of void fraction signals at a given scale on the joint time–frequency diagram. The void signals are processed with Continuous Wavelet Transform (CWT) to get the local wavelet energy coefficients map on the time–frequency diagram. The effective local wavelet energy and the effective scale are then calculated. Then the criteria for flow pattern identification are, finally, obtained. A series of void fraction measurements were conducted over a wide range of air–water vertical-upward flow condition to provide an extensive database to cover several types of flow patterns. The results show that the proposed method has a high precision for characterizing different flow regimes in two-phase flow, and is considerably more promising for the online recognition of two-phase flow patterns due to the short time of data processing.

1. Introduction

The two-phase gas–liquid flow regime map plays an important role in advanced energy conversion systems and modern industrial processes since the characteristics of the two-phase flow and heat transfer are strongly dependent on the flow regimes. A clear understanding of the multi-dimensional phenomena on the two-phase flow is crucial, especially, to the development of advanced nuclear reactor systems and their safety analysis (Song et al., 2007). Therefore, an accurate identification of the flow regime is essential for understanding and predicting the behavior of flow systems under a variety of operating conditions.

A flow regime or *flow pattern* is defined as the morphological arrangement of the components in a multi-phase flow. Conventionally, a flow pattern is often obviously recognized from visual or photographic observations, but is not adequate for defining the regime objectively with completeness because of the complicated nature of its phasic interfaces (Wallis, 1969). Even when using high-speed photography, the picture captured from the visualization method is often confusing and difficult to interpret, especially when dealing with high speed flows. In addition, there are systems in which the flow channel is opaque and flow visualization is impossible. Taitel et al. (1980) have shown that there is little agreement among the various published flow regime maps due to the subjectivity of the observer involved in distinguishing the differences in the flow patterns.

Some other methods have been proposed in an attempt to more objectively classify flow patterns using the extraction of characteristic variables from the signal of the two-phase flow, such as fluctuations of void fraction or differential pressure, which are supposed to reflect the flow configuration (Jones and Zuber, 1975; Barnea et al., 1980; Vince and Lahey, 1982; Tutu, 1982; Matsui, 1986; Costigan and Whalley, 1997). Analyses of the fluctuation signal have typically been made by using the fast Fourier transform (FFT) and statistical methods to correlate the void fluctuation signal with the observed flow phenomena. The characteristics of peak values and the shape of the probability density function (PDF) or power spectral density function (PSD) of the measured time series have been previously utilized to identify the flow regime. It has been suggested that the classification of two-phase flows in vertical tubes be structured in such a way that there would be three dominant patterns which consist of the bubbly, slug and annular regimes. It has been shown that the PDFs for bubbly and annular flows exhibit a single peak corresponding to the low and high value of gas void fraction, respectively, whereas a slug flow is characterized by a bimodal PDF with a low-void peak corresponding to the liquid slug passage and a high-void peak due to the Taylor bubble.

* Corresponding author at: Korea Atomic Energy Research Institute, Daedeok-daero 1045, Yuseong, Daejeon 305-353, Republic of Korea. Tel.: +82 42 868 8876; fax: +82 42 868 8362.
E-mail address: chsong@kaeri.re.kr (C.-H. Song).

0301-9322/$ - see front matter © 2010 Elsevier Ltd. All rights reserved.
doi:10.1016/j.ijmultiphaseflow.2010.04.007

However, the signal to be analyzed must have sufficient length to yield statistically significant estimates of the characteristic parameters which require the additional restriction on the stability of a flow. In addition, it is very difficult to objectively identify the flow regime transition in which the flow structure is highly oscillatory and gradual developing along a flow channel. Chaotic oscillations are the random-like motions emerging from completely deterministic systems. With the new discoveries in nonlinear dynamics as well as their new concepts and tools for detecting chaotic vibrations in physical systems, some applications of chaos analysis on flow regime identification have been studied (Van den Bleek and Schouten, 1993; Letzel et al., 1997; Lin et al., 2001; Nedeltchev et al., 2006, 2007).

Some other efforts in digital signal processing have introduced many new approaches for describing the local features of the signal representing a two-phase flow. The time-scale (frequency) analysis, made possible by the wavelet transform, provides new insight into the characteristics of the signals through the time–frequency maps of a time-variant spectral decomposition that conventional approaches can not obtain. The wavelet transform has been widely used in signal processing and has been shown to be a useful tool for the analysis of non-stationary and transient signals due to its localization properties in the time domain. At present, the wavelet analysis technique has been widely and successfully applied in the research of two-phase flow: Seleghim and Milioli (2001) used wavelet de-noising techniques to determine the bubble sizes in two-phase flow. Kulkarnia et al. (2001) employed wavelet to measure the fraction of gas in a bubble column flow. Wu et al. (2001) used a wavelet theory to denoise and analyze the signals of pressure in a oil–gas–water multi-phase flow, and Shang et al. (2004) used a wavelet signal extraction technique to investigate the instability of two-phase flow.

The applicability of a wavelet analysis technique to the flow regime identification has been demonstrated by Kirpalani et al. (2001), who applied the Continuous Wavelet Transform (CWT) to the analysis of the time series of wall pressure fluctuations in various patterns of two-phase flow. They have shown that the wavelet spectrum of the measured signal contains some features that are similar to the PSD of the wall pressure time series measured by Hubbard and Dukler (1966). It has been confirmed that the wavelet transform coefficients incorporate the features of a PSD and, consequently, can be used for flow regime identification. Elperin and Klochko (2002) showed that the measured time series of dynamic pressure fluctuations can contain noises originating from some other sources than the test section, such as pump fluctuations and flow loop vibrations, and they applied the Discrete Wavelet Transform (DWT) using experimental data on the time series of differential pressure across a Venturi meter in order to eliminate these influences. They found that the distribution of a wavelet variance vector, which is referred to the wavelet spectrum, over the scale (frequency) is shown to contain valuable information regarding the hydrodynamic characteristics for a two-phase flow regime to be considered. Since the estimation of the wavelet coefficients does not require large-sized sample, the proposed method might be used for the on-line identification of flow regimes in two-phase flow systems, and might also be implemented with any measurement device (provided its output is related to the gas fraction of a flow). However, these previous studies have examined only the potential of applying the wavelet analysis technique for the flow patterns recognition, but none of them proposed a concrete method of identifying the flow patterns and their transition in two-phase flow.

In particular, the fluctuations of void fraction can reveal the characteristics of the structures of the discrete phase in two-phase flow. Among the measuring methods of void fraction, the Impedance Void Meter (IVM) is definitely of practical use due to the non-intrusiveness of sensors, relatively simple measuring principle and reasonable cost for signal processing (Delhaye et al., 1987). Song et al. (1995, 1998) have confirmed that the IVM has a good dynamic resolution, which is required to investigate the structural developments of two-phase flow and the propagation of void waves in a flow channel. The goal of the present study is to develop some objective indicators utilizing the CWT technique for flow patterns identification based on the interrelation between void fluctuations measured by IVMs and the flow patterns in a vertical-upward air–water flow condition. Moreover, the local features of the void signal can be represented in terms of the local wavelet energy coefficients map which can indicate the structural developments of two-phase flow and its use for the on-line flow pattern recognition.

2. Experimental setup

The vertical air–water loop (VAWL) has been used for investigating the transport phenomena of two-phase flow at Korea Atomic Energy Research Institute (KAERI). A schematic diagram of the test facility is shown in Fig. 1. This test loop consists of a test section, bubble generator, water supply system, air supply system and a data acquisition system. The test section is made of a transparent acryl pipe with a diameter of 0.08 m and a height of about 10 m. The main water flow is supplied in the two different parts of the bubble generator, which is located at the inlet of the test section. A part of the water in-flow is injected into the bubble passage outside the gas chamber in the bubble generator to control the bubble size to be produced, whereas the major part of the water flow is injected directly into the test section without passing through the bubble passage. Air is also injected into the central region of the bubble generator and then mixed with the injected water and enters the test section (Song et al., 1995). The flow of injected air is controlled by a regulating valve. The total water flow, bypass water flow, and air flow are measured by Coriolis mass flow meters. The measurement error of mass flow is less than 0.2% of the whole flow range. In order to measure the temperature of flow in the test section, a resistance temperature detector (RTD) is installed at the entrance region of the test section. Even though the test loop is being operated under ambient flow conditions, the RTD is used to control the flow temperature and as a result to reduce the variation of conductivity of the fluid due to a temperature variation. By referring to the temperature signal, the pre-heater which is installed at the upstream of the test section and the cooler in the storage tank are operated to maintain the system with a constant temperature. In order to measure the pressure of the test section, one pressure transmitter (PT) and one differential pressure transmitter (DPT) are used. The system pressure can be stably maintained by a finely adjustable needle valve installed at the top of the water storage tank for controlling the system pressure.

An improved IVM with multi-channels have been developed by Song et al. (1995, 1998) for measuring the channel-averaged void fraction as shown in Fig. 2. Its measuring principle is basically based upon the differences in electrical conductance between each phase in a two-phase flow mixture due to the variation of void fraction around a void sensor. The multi-channel IVM is composed of a main sensor which has three channels, a reference sensor and a signal processing unit. Each channel of the main sensor consists of two measuring electrodes and four guard electrodes, and is flush-mounted to the inner wall of the test section to avoid flow disturbances. The arc ratio of the electrode portion is half of the inner circumference of the flow channel, as recommended by Tournaire (1986). Two guard electrodes installed on each side of the central electrode are installed to ensure that the electric field is uniform in the measuring volume. Both the measuring electrodes and guard electrodes are excited by the same frequency of 20 kHz with which the portion of capacitance in the measured impedance is negligible. A reference sensor is installed upstream of the bubble genera-

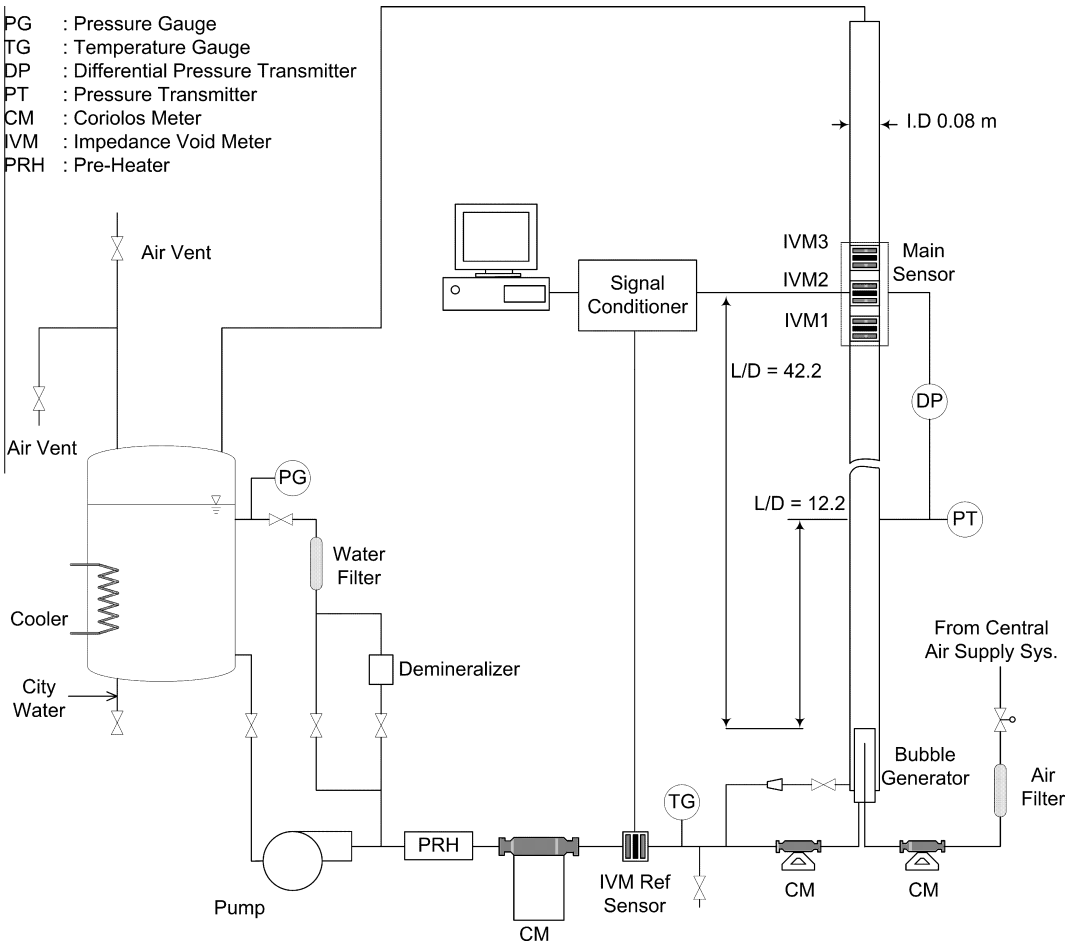

Fig. 1. Air–water test loop (VAWL).

tor, where only water flows, as shown in Fig. 1, in order to eliminate the drift in void signals caused by the changes in electrical properties of flow medium. In the signal processing unit, a main sensor signal is normalized by the reference sensor signal to compensate a time-dependent variation of the conductivity of flow medium. Therefore, a unique factor to affect the electrical properties at the location of a main sensor is the variation of gas fraction, i.e., the void fraction. The relative short width (0.01 m) of a measuring electrode is used for obtaining sufficient sensitivity to small changes in void fraction. The distance between two successive main sensors is chosen to be 0.07 m to meet the necessity of distinguishing void fluctuations with a relatively long wavelength. The multi-channel IVM is installed axially at a location L/D = 42.2. The detailed design features, the principle of signal processing and the calibration method can be found in previous studies (Song et al., 1995, 1998; Euh, 2002).

The data acquisition system is comprised of a signal conditioner, 16-bit A/D converter board and a personal computer. The void fraction is recorded at 300 Hz. All the A/D boards are installed in a PC. In the present measurement, a series of tests is performed at 0.2 MPa and 313 K of the system condition under the following flow conditions in the test section:

- Liquid superficial velocity: J_f = 0.18, 0.275, 0.45, 0.675, 1.0 m/s.
- Gas superficial velocity: J_g = 0.01 – 1.8 m/s.

A wavelet spectral analysis of the collected void fraction was carried out using the software developed based on the MATLAB®. Consecutive 10-s intervals of void fraction were analyzed to get the wavelet analysis results. The sampling period of 10 s give the good results and the time processing is less than 1 s. Moreover, with sampling period of 10 s, we can easily recognize the local behavior of void signal.

3. Definition of flow patterns

In order to identify the flow patterns using void signals measured from the IVM, it is important to define each flow pattern under consideration clearly. When a gas–liquid mixture flows upward in a vertical tube, the two-phases may distribute in a number of configurations, each of which characterizes the radial and axial distribution of the liquid and gas phases. The void signal to indicate flow is quite random and provides some ambiguity in objectively discriminating the transition from one to another in a deterministic way when relying on existing method of signal analysis. The basic flow patterns defined by Hewitt and Hall Taylor (1970), which are bubbly flow, slug flow, and churn flow, have been used and analyzed in this study.

In the *bubbly* flow, the gas phase is rather uniformly distributed in the form of discrete bubbles in a continuous liquid phase. From the statistical analysis of void signals, however, it has been found that the two distinct modes of flow structural developments in the bubbly flow are observed, which are dependent on the bubble size (Song et al., 1995).

- *Discrete bubbly flow*: The gas phase is distributed as discrete bubbles, as shown in Fig. 3a where the void fluctuations remain relatively small in time record.

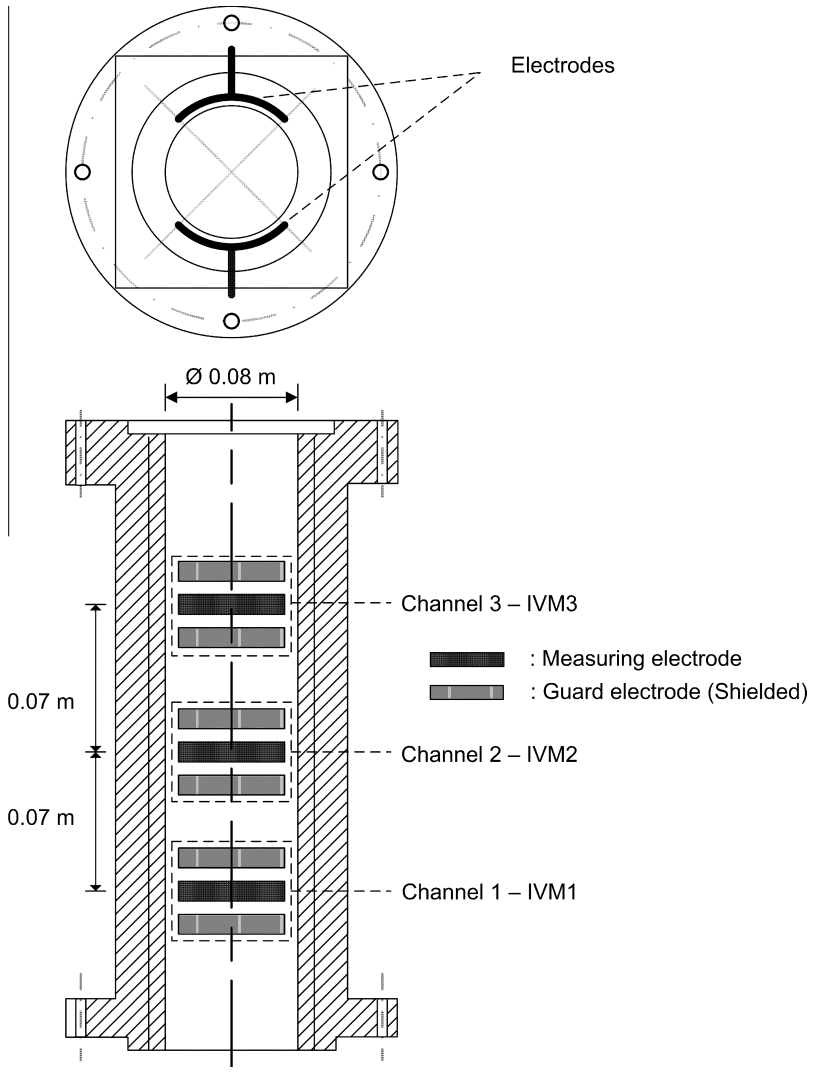

Fig. 2. Cross section of the main sensor.

- *Clustered/cap bubbly flow*: This flow consists of the bubble clusters, flowing in the center of the flow channel, and the discrete bubbles flowing near the channel wall and between successive bubble clusters. The bubble clusters become larger and the bubbles in the clusters coalesce with each other to form cap bubbles while passing through the flow channel. The clustered/cap bubbly flows are well indicated in Fig. 3b by the void fluctuations with large amplitude, which indicate the passage of a cap or clustered bubbles across the void probe.

The *Slug* flow is defined as follows: Most of the gas is located in large bullet-shaped bubbles, called the Taylor bubbles, of which the diameter is similar to the pipe diameter. Taylor bubbles are separated by the slugs of continuous liquid which bridge the pipe and contain small gas bubbles. Between the Taylor bubbles and the pipe wall, liquid flows downward in the form of a thin film (Taitel et al., 1980). A typical shape of the time series of void fluctuation for the slug regime is shown in Fig. 3c. This figure is characterized by rather periodic peaks with high-amplitude, which indicate the alternating passage of a large bubble with high void fraction and the liquid slug with entrained bubbles with low void fraction.

The *Churn* flow is somewhat similar to the slug flow. It is, however, much more chaotic, frothy and disordered. Duckler and Taitel (1986) as well as Taitel et al. (1980) treat churn flow as an entrance phenomenon. They consider it as a part of process for the formation of stable slug flow further downstream in a pipe. According to them, at the inlet where gas and liquid slugs are introduced, short liquid slugs and Taylor bubble are formed. However, since short liquid slugs are unstable, they collapse down the tube, coalesce with the next slug and form a bigger slug which is able to retain its identity longer before it too collapses. If the pipe is long enough, this merging and collapse of successive slugs will ultimately lead to liquid slugs long enough to become stable. The flow in the intervening region (i.e., that between the entrance and the point where stable slugs are formed) appears to be churn flow because of the oscillatory motion of the rising and collapsing liquid (see Jayanti and Hewitt, 1992). As described in Hewiit and Jayanti (1993), "Churn flow" is an intermediate region between slug flow and annular flow. This regime has been recognized as a regime of fully developed flow, occurring even in very long tubes. It has been delineated by many authors in the literature (e.g., Hewitt and Hall Taylor, 1970; Song et al., 1995). The time series of the void signal in Fig. 3d shows a typical characteristic of churn flow.

4. Wavelet analysis technique

Wavelet transform is introduced in detail in an online Supplement data. Generally speaking, the wavelet transform is a tool that

divides up the data, functions, or operators into different frequency components and then analyzes each component with a resolution matched to its scale (Li et al., 2002). The essential difference between the wavelet and Fourier analyses is that the wavelet basis function for any frequency band consists of a number of local functions strung together, each with its own amplitude, and can thus distinguish local events at different times at the same frequency.

4.1. Discrete Wavelet Transform (DWT)

The most efficient and compact form of wavelet analysis is accomplished by decomposing a signal into a subset of translated and dilated mother wavelets, where these various scales and shifts in the mother wavelet are related based on powers of two. A full representation of the signal can be achieved by using a vector of wavelet coefficients with the same length as the original signal.

The family of analyzing wavelets can be written as follows:

$$\psi_{i,j}(t) = 2^{i/2}\psi(2^i t - j) \tag{1}$$

For the signal $x(t)$, the DWT is

$$w_{i,j} = w_{2^i+j} = \sum_t x(t)\psi_{i,j}(t) = \sum_t x(t)\psi(2^i t - j) \tag{2}$$

and the corresponding inverse wavelet transform IWT is

$$x(t) = \sum_i \sum_j w_{i,j}\psi_{i,j}(t) \tag{3}$$

4.2. Continuous Wavelet Transform (CWT)

While the DWT is the most efficient and compact, its power of two relationships in scale fixes its frequency resolution. It is often desirable to differentiate between smaller frequency bands than DWT allows. This is achievable by using the scales that are more closely spaced together than the 2^i relationship, which is the basis for the CWT.

The CWT is defined on the basis of a family of analyzing wavelets, $\psi_{a,b}(t)$, that are generated by varying the dialitions or scales, a, and translations, b, from a mother wavelet, $\psi(t)$, as:

$$\psi_{a,b}(t) = \frac{1}{\sqrt{a}}\psi\left(\frac{t-b}{a}\right) \tag{4}$$

where $a > 0$, $-\infty < b < \infty$.

In Eq. (4), the wavelet function must be satisfied by the admissibility condition:

$$\int_{-\infty}^{+\infty} \psi(t)dt = 0 \tag{5}$$

The wavelet transform of the finite energy temporal signal $x(t) \in L^2(R)$ is the joint time-scale function, defined as follows (Daubechies, 1992):

$$w_{a,b} = \int_{-\infty}^{+\infty} x(t)\psi_{a,b}dt = \frac{1}{\sqrt{a}}\int_{-\infty}^{+\infty} x(t)\psi\left(\frac{t-b}{a}\right)dt \tag{6}$$

The space-scale locality of the analyzing wavelet ψ leads to the conservation of locality in the wavelet coefficient space. For instance, if ψ is well-localized in the space interval Δt for $a = 1$, then the wavelet coefficients corresponding to the position t_0 will all be contained in the influence cone defined by $t_0 \in \left[t_0 - \frac{a\cdot\Delta t}{2}, t_0 + \frac{a\cdot\Delta t}{2}\right]$. This cone corresponds to the spatial support of all dialated wavelets at the point t_0 (Farge, 1992).

5. Results and discussion

5.1. Choice of the analyzing wavelet

There are a variety of mother wavelets available in the literature, each of which has been developed to meet certain specific criteria. The effectiveness of the wavelet analysis strongly depends upon the choice of the mother wavelet. Elperin and Klochko (2002) have showed the difficulty of choosing the wavelet which will compose the best basis for any measured signal because the characteristics of the signal are flow-regime-dependent: the wavelet suitable for the slug flow signal, for instance, will not fit the signal measured in a churn flow. They have compared the performance of well-known basic wavelets in terms of some preset criterion provided by the statistical information theory, e.g., entropy or sparsity. The best basis of wavelets for a given signal satisfies that the specified criterion evaluated for the wavelet decomposition coefficients attains the minimum value. Based on this criterion, Daubechies's least symmetric wavelet of order four, which reduces the sparsity by 40% on average with respect to the time domain representation, was chosen in their study for the analysis of the time series of differential pressure using DWT.

For CWT, the parameters vary in a continuous fashion. This representation offers the maximum freedom in the choice of the analysis wavelet. Continuous analysis is often easier to interpret, since its redundancy tends to reinforce the traits and makes all information more visible. The scale may be selected over any range the user desires. Hence, CWT does not need to contain information over the complete range of frequencies contained in the signal. The user may select a very narrow range of scales to isolate and pull details from a particular frequency band. Daubechies's wavelet was chosen in the present study for the analysis of the time series of void fluctuation using the CWT.

5.2. Local wavelet energy coefficient

The wavelet coefficients, $w_{i,j}$, can be utilized in a variety of ways to draw out useful signal information. Farge (1992) showed that a common pitfall in interpreting wavelet coefficients is to link their strength to the signal's strength, whereas they actually correspond to variations in the signal at a given scale and a given point. If the signal does not oscillate at a certain scale and position, then the corresponding wavelet coefficients are zero. Hence, wavelet coefficients may be used to derive an estimate of the power spectrum, and also provide the scalogram which describes the signal energy on a time-scale domain. This facilitates the identification of time-varying energy flux, spectral evolution, and transient bursts not readily discernible using time or frequency domain methods.

Particularly in two-phase flow, the information on void fraction can reveal the characteristics of the structures of the discrete phase in two-phase flow and they are well-correlated with flow patterns. The typical void signals obtained from the IVMs are described in terms of void fraction peaks which indicate the passage of large void structures across the void probe such as clustered bubbles, cap bubbles, Taylor bubbles, elongated and distorted bubbles, followed by liquid slugs containing discrete bubbles (Fig. 3). Therefore, the information about these void fraction peaks such as their amplitudes and widths are essential to represent flow patterns. The amplitude is considered as a difference in void fraction between large void structures and the liquid bridge containing discrete bubbles. To utilize the wavelet analysis technique on this aspect, the wavelet coefficients are used to derive the local wavelet energy (LWE) coefficients. This parameter can be interpreted in such a way that it is proportional to the square of amplitude of

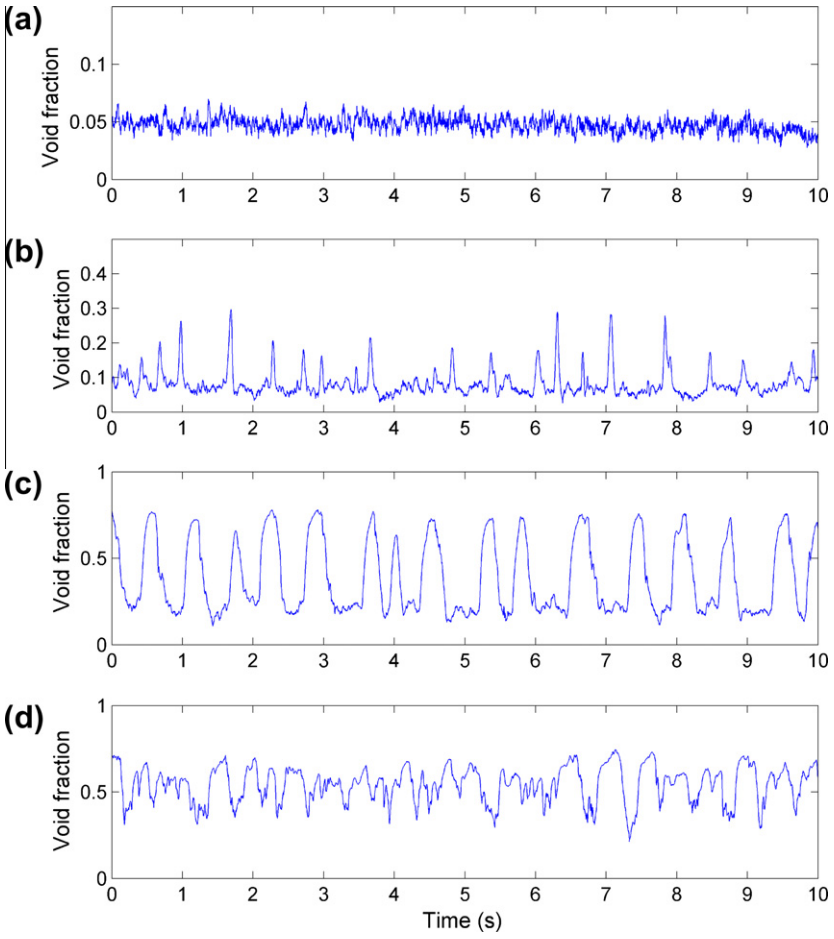

Fig. 3. Typical signals obtained from IVMs: (a) Discrete bubbly flow, (b) clustered/Cap bubbly flow, (c) slug flow, and (d) churn/turbulent flow.

fluctuations at a given scale and it has been successfully used in the application of wavelet technique to turbulence (Farge, 1992).

The LWE coefficients can be defined as follows:

$$W_{a,b} = \frac{\left|w^2_{a,b}\right|}{a} \tag{7}$$

The LWE coefficients are well suited for analyzing non-stationary events such as transient and evolutionary phenomena and they are used for time-scale signal representation, the so-called *LWE coefficients map*. Since the void fraction peaks are positive peaks, so the positive value of wavelet coefficients were used for calculating the LWE coefficients. Examples are given in Fig. 4 in order to demonstrate the applicability of LWE coefficients. In this figure, the single-peak signals were simulated based on sinusoidal functions with different amplitudes and periods. The signals were processed using the CWT transform to produce the LWE coefficients map. In the LWE coefficients maps, the values of local wavelet energy coefficients are represented by color and they can be interpolated by the color bar given on the right side of these maps. The scale values corresponding with LWE coefficients are indicated directly on the scales axis. The maximum LWE coefficient and the corresponding scale are determined by using peak-finding algorithm in MATLAB®. Fig. 4a and b shows the signals with the same width and different amplitudes, resulting in the LWE coefficients map with two peaks located at the same scale but different in maximum LWE coefficients. These values are well proportional to the square of signal amplitudes. Fig. 4a and c shows the signals with the same amplitude and different widths resulting in the LWE coefficients map with two peaks located at different scales with the same value of maximum LWE coefficient. These scale values are well proportional to the width of signals. Figs. 4b and d shows that the results are not dependent on the base level of signals. Fig. 5 shows the excellent correlation which is obtained by a thorough simulation process between maximum LWE coefficient and the amplitude of signal. Hence, the LWE coefficients map provides very useful information about the characteristics of void fraction peaks.

When the gas flow increases, the large void structures, such as Taylor bubbles, are expected to appear at a void sensor more frequently and the distance between two successive peaks in time-dependent signals become closer. On a given scale, this closer space may lead to the overlap between the influence cones of nearby peaks so that the maximum LWE coefficients and corresponding scales in a time-scale map could underestimate or overestimate the amplitude and width of signals. This phenomenon happens even more strongly at the slug-to-churn transition flow condition. This kind of influence has been exhaustively investigated in order to make the prediction method meaningful and applicable. Fig. 6 illustrates some of the typical cases. Error estimation is explained in detail in an online Supplementary material. The results show that the relative error of the prediction is less than 15%.

5.3. Objective indicators for flow pattern identification

A series of tests was conducted extensively on the VAWL test facility at KAERI aiming at revealing the objective indicator for two-phase flow pattern identification. The time series of void frac-

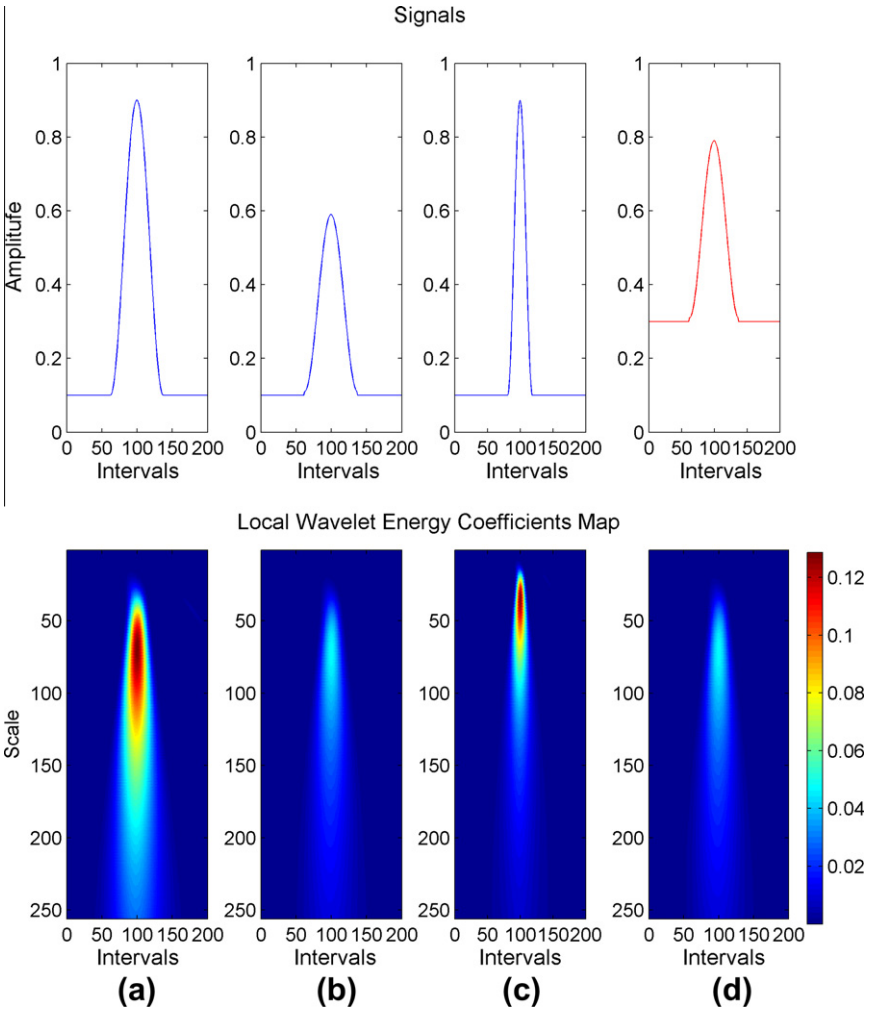

Fig. 4. Examples of LWE coefficient map.

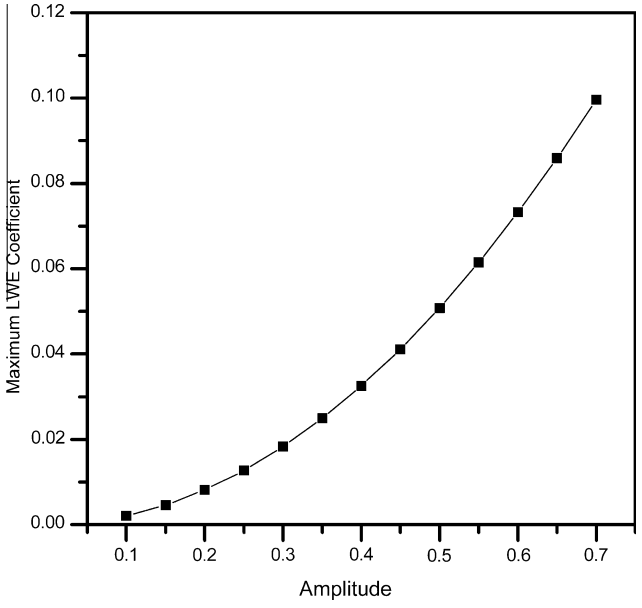

Fig. 5. The correlation between maximum LWE coefficient and signal amplitude.

tion for 10 s have been processed using the CWT transform to produce the LWE coefficients map.

In a discrete bubbly flow, as typically shown in Fig. 7, the void fraction at a measuring position fluctuates around its mean value as bubbles pass through the probe. The time record shows random-like fluctuations with very small amplitude and the LWE coefficients map shows some peaks located at small-scale with very small LWE coefficient ($\sim 10^{-5}$). A clustered/cap bubbly flow, as typically shown in Fig. 8, flows with a large bubble size forms bubble clusters even at low void fraction. Bubble clusters become larger and the bubbles in the clusters coalesce with each other to form cap bubbles while passing through the channel. The time series shows some single peaks void fraction and these peaks are well illustrated in the LWE coefficients map with peaks located at a medium scale and larger LWE coefficient ($\sim 10^{-3}$). In slug flow, as typically shown in Fig. 9, the characteristic of time series comprises alternating intervals characterizing the bubbly and annular flows which resulted in a large void fraction peak and width. This is well presented in the LWE coefficients map with regular peaks located at high scale value and large LWE coefficient ($\sim 10^{-2}$ to 10^{-1}).

When a gas flow increases, visual observations made through the tube wall suggest, as shown in Mao and Dukler (1993), that the flow becomes chaotic in nature. That is, the readily observable well-defined slug and Taylor bubble lengths are no longer clearly discernible through the tube wall. The position of the front of the bubble or slug, which is moving uniformly upward, becomes oscillatory in nature and one seems to see large lumps of liquid moving downward as well as upward. This oscillatory behavior displays

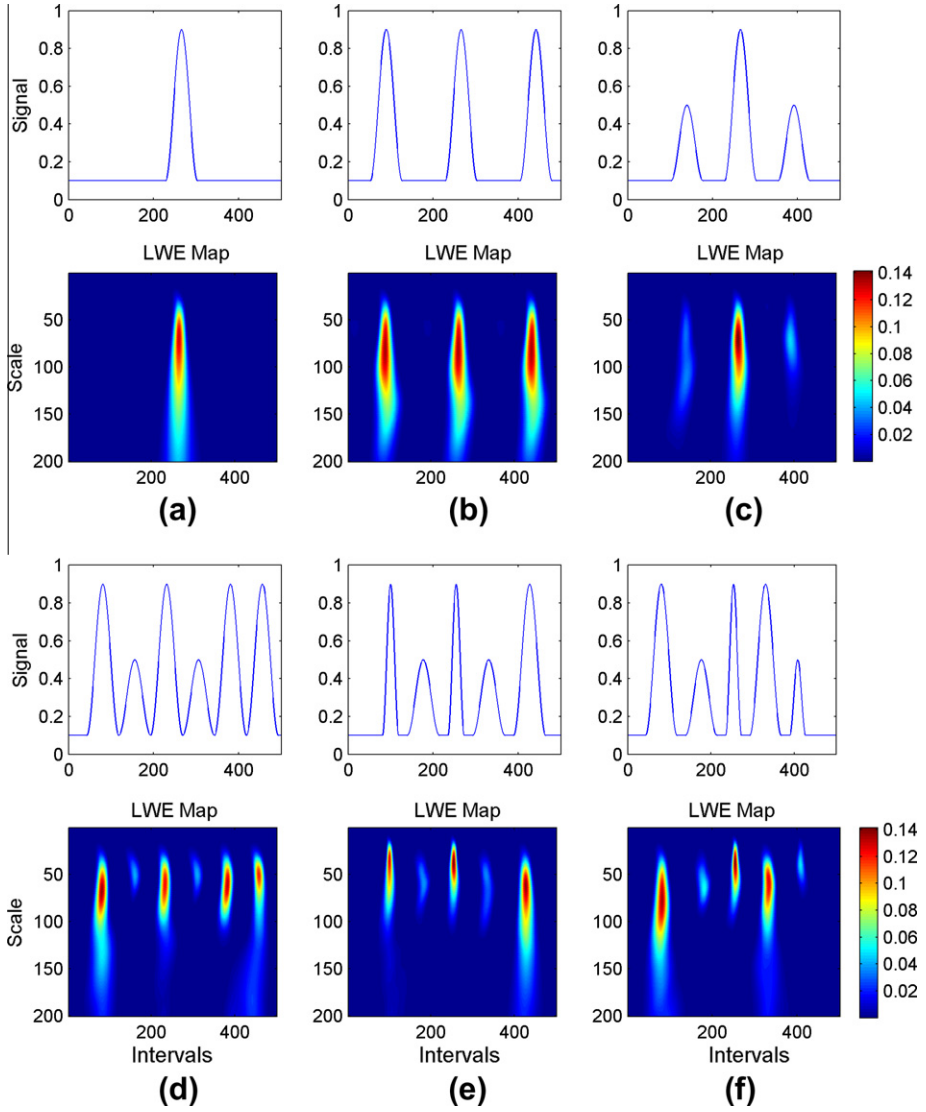

Fig. 6. Examples of influence cone effects.

over the irregular periods. This feature of churn flow is shown in Fig. 10. In the LWE coefficients map, the peaks are distributed in broad range of scale and lower LWE coefficient ($\sim 10^{-3}$ to 10^{-2}) when compared with the slug flow.

From these results, it is reasonable to use two values of peaks in the LWE coefficients map as the objective indicators for flow pattern identification. At given steady state flow condition, however, void fraction signals of a certain length contain a number of peaks with different amplitudes and corresponding widths because of the complex and chaotic nature of two-phase flow. Hence, the effective LWE and effective scale were derived in order to represent the behavior of void fraction signal which correlates with the flow pattern. The effective scale is weighted by LWE coefficients taking into account the level contribution based on energy.

The effective LWE coefficient and the effective scale are defined as:

$$W^* = \frac{1}{N}\sum_{k=1}^{N} W_k \tag{8}$$

$$a^* = \frac{\sum_{k=1}^{N} a_i W_k}{\sum_{k=1}^{N} W_k} \tag{9}$$

where N is the number of peaks in the LWE coefficients map and W_k is the maximum LWE coefficient at peak k.

The large void structure length can be well represented by the effective scale value. However, it strongly depends on the propagation speed of large void structure along the test section. It is reasonable to estimate the effective length of large void structure in such a way that the length is proportional to the propagation speed and the value of effective scale. The relation is defined as:

$$L_e = V_p a^* \Delta t. \tag{10}$$

The propagation speed, V_p can be estimated as follows:

$$V_p = \frac{\Delta z}{\tau_{\max}} \tag{11}$$

where Δz is the distance between two successive void probes, and τ_{max} is the time-lag.

For the estimation of a time-lag, the cross-correlation function (CCF) has been commonly used in the literature. Cross-correlation is a measure of the similarity of two time-dependent signals as a function of a time-lag applied to them. The time-lag is estimated by the peak time of CCF. In the present study, the void signals are acquired from three consecutive IVM channels and the LWE coefficient maps are generated by using the CWT transforms. These maps can be used to estimate not only the time-lag, but also the dispersive properties of void waves. Nevertheless, in discrete bub-

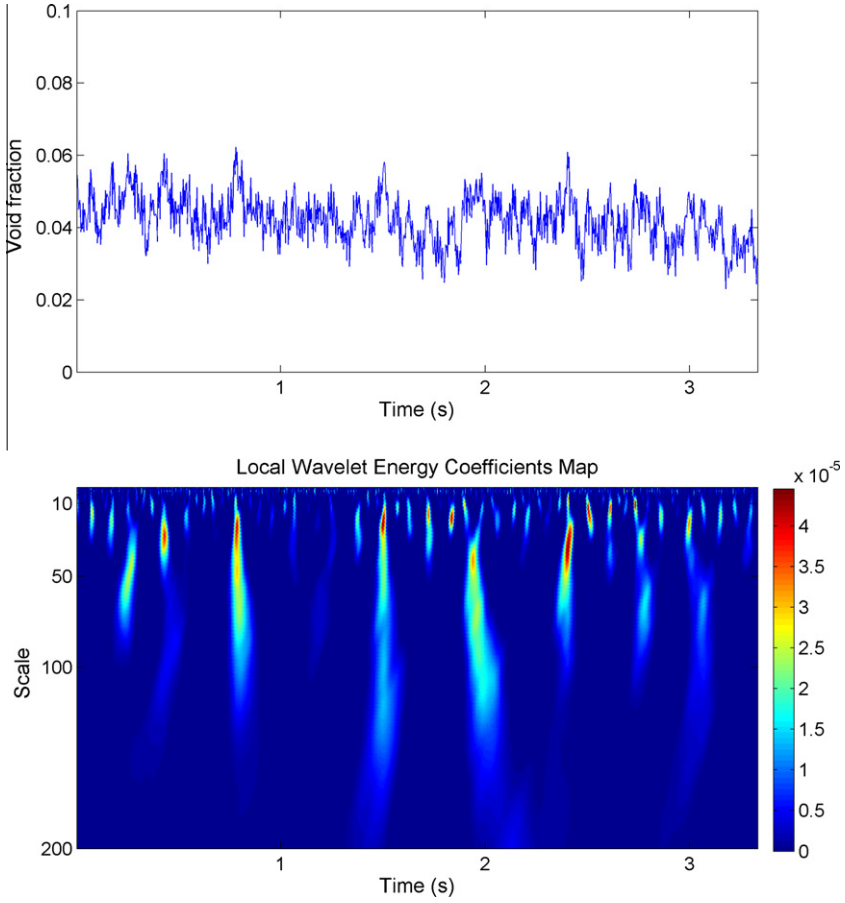

Fig. 7. Typical signal of discrete bubbly flow.

bly flow, the stochastic nature of the distribution of discrete bubbles along the flow and their random motion make the CCF inapplicable. In this case, the mean value of void fraction is used together with the effective LWE coefficient to characterize the discrete bubbly flow pattern.

The uncertainty of propagation speed can be estimated in advance as follows (Fagundes Netto et al., 1999):

$$\frac{dV_p}{V_p} = \pm\frac{2}{\Delta z}\frac{V_p}{f} \tag{12}$$

where f is the sampling frequency.

As we can see in the estimation equation, this uncertainty can be reduced as small as we can by increasing the sampling frequency f. With the flexibility of our data acquisition system, we can easily increase the sampling frequency up to 10,000 Hz or greater. However, as we mentioned before, an increase of sampling frequency will lead to an increase in signal processing time with Wavelet transform. Our goal is to achieve the results in short time with acceptable level of confidence. Hence, the propagation speed with an uncertainty up to 10% is acceptable. Once the time processing is not considered, the frequency should be increased in order to reduce the uncertainty of propagation speed.

Therefore, some objective indicators for the flow pattern identification have been proposed as follows:

- The effective local wavelet energy (LWE^*)

$$LWE^* = W^* \tag{13}$$

- The effective length to diameter ratio (LDR)

$$LDR = \frac{L_e}{D} = \frac{V_p a^* \Delta t}{D} = \frac{V_p \Delta t}{D}\frac{\sum_{i=1}^{N} a_i W_i}{\sum_{i=1}^{N} W_i} \tag{14}$$

where D is diameter of tube.

- The mean value of void fraction (MVF)

5.4. Rule of Identification Method

Fig. 11 shows the map of 90 test conditions covering several types of flow patterns which were constructed based on two parameters LWE^* and LDR. A hundred tests at each flow condition have been evaluated in order to test the repeatability of the results. This map is divided into three zones which clearly show the differentiation among different two-phase flow patterns.

In the case of a discrete bubbly flow, the value of LWE^* coefficient is very small ($\sim 10^{-5}$) so that they can not be displayed in the map. As mentioned in Section 5.3, the MVF and the LWE^* coefficient are used to characterize a discrete bubbly flow. Experiments were conducted at different liquid velocities in order to set the criteria for differentiating the discrete bubbly flow and clustered/cap bubbly flow. The results show that the LWE^* coefficient of 10^{-4} is acceptable in most cases when the MVF is less than 0.2.

As investigated by many researchers (see Taitel et al., 1980; Mishima and Ishii, 1984), the transition from a bubbly flow to a slug flow in a tube occurs mainly due to gradual agglomerations and coalescences of smaller bubbles into cap bubbles. Once a cap bubble is formed, further coalescences follow in the wake region of a cap bubble. With the increases in gas flow, the cap bubble should be elongated and eventually developed into the

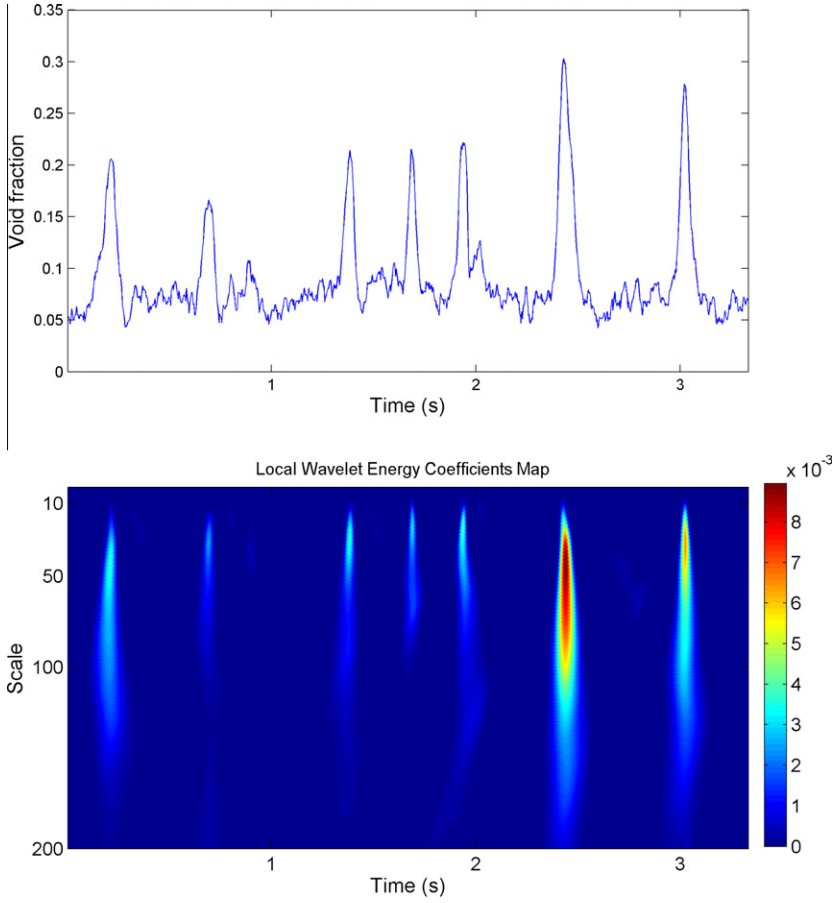

Fig. 8. Typical signal of cluster/cap bubbly flow.

Taylor bubble. This process is well-presented in the Zone-1 of Fig. 11 which shows the trend curves at different liquid velocities with the gradual increase of the LWE^* coefficient and corresponding *LDR* value. The trend curves are located quite closely which shows that the effect of turbulent fluctuations associated with the flow is small in the forming process of cap or Taylor bubbles. However, the Zone-2 of Fig. 11 shows the differences when the gas flow is continuously increased. At a low liquid velocity, the process of coalescence could be maintained in order to form larger Taylor bubbles. As the liquid velocity is increased, the effect of turbulence becomes more significant and it can prevent the coalescence and forming process of Taylor bubbles. Even in this case, the cap bubbles are not large enough to occupy the cross-section of the pipe so as to cause slug flow in the manner described in Section 3 (though the length of the bubble is increased). Moreover, the turbulent forces can act to break and disperse the gas phase into small bubbles inside the liquid slug which results in decreasing void fraction peaks and the LWE^* coefficient.

The bubbly-to-slug transition has been thoroughly studied by many researchers. Taitel et al. (1980) carried experiments using a vertical tube with a 0.05 m and 0.025 m I.D. in upward gas–liquid flow at low gas flow rates and they observed the large cap bubbles having a diameter nearly that of the tube, with lengths of 1–2 diameters at the transition to slug flow. Costigan and Whalley (1997) measured dynamic void fraction using conductivity probes in a vertical 0.032 m diameter tube to identify the slug regime and they proposed some criteria of flow pattern identification as follows:

- A *Stable* slug flow exists when liquid slugs with void fractions up to 0.4 are separated by Taylor bubbles with void fractions of 0.8 or more.
- An *Unstable* slug flow occurs at relatively high liquid velocities. It is characterized by liquid slug void fractions which are higher than 0.4 merging with Taylor bubble void fractions which are lower than 0.8.

As mentioned in the Introduction Section, a flow regime or flow pattern is defined as the morphological arrangement of the components in a multi-phase flow. Part of the problem arises from the lack of agreement in the description and classification of the flow patterns and the subjectivity of the observer (Taitel et al., 1980). For example, what are the criteria for discrimination between cap bubble and Taylor bubble? It is quite difficult to find the best answer for this question. Based on some works referred in the paper, we proposed the criteria for discrimination based on the length of bubble and the difference in void fraction between the gas bubble and liquid slug. It is such a kind of morphological arrangement of gas and liquid in pipe. To objectively identify the flow patterns and based upon the definition of slug flow pattern, we consider the elongated or cap bubble as Taylor bubbles if it satisfies the following two conditions:

- The minimum bubble length is twice the pipe diameter.
- The minimum difference in void fraction between cap bubble and liquid slug is 0.45.

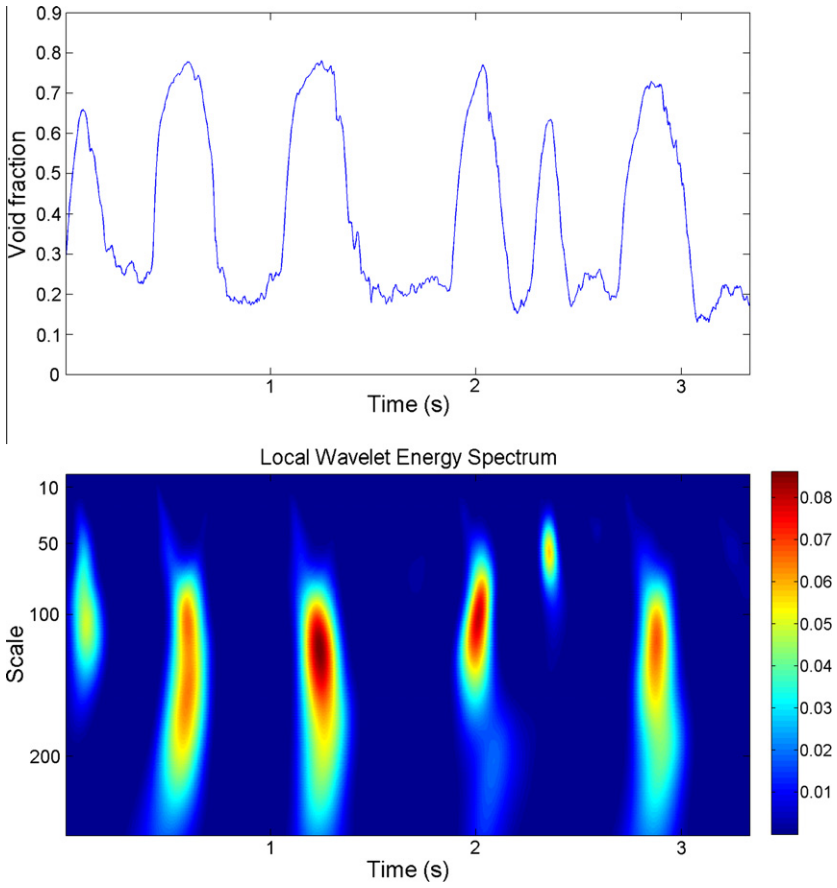

Fig. 9. Typical signal of slug flow.

The value of 0.45 can be correlated with the LWE^* coefficient based on the calibration curve which is obtained from the signal simulation in Section 5.2. The accurate correlation, particularly, between the length of bubbles to diameter ratio and *LDR* need further studies to correctly set the criteria. In the present study, based on the good dynamic characteristic of IVMs, the value of 2.0 is proposed for the *LDR* value in order to differentiate between the cap bubbly flow and the slug flow.

As investigated by Costigan and Whalley (1997), liquid slugs begin to collapse when their void fractions are in the 0.35–0.45 region, and the excess of 0.4 is indicative of the fact that slugs are collapsing. Moreover, aerated liquid falls in the tube causing the bubble void fraction to fall significantly. As a consequence, the difference in void fraction between Taylor bubble and the liquid slug is decreased. The Zone-3 of Fig. 11 shows clearly the LWE^* coefficient decreases when the gas flow continuously increases. Although some slugs are collapsing and there are obvious chaotic oscillations in the flow, other slugs still have sufficient momentum to traverse the length of the test section, and it is difficult to decide whether to classify this type of flow as slug or as churn, since it exhibits some characteristics of both. In our works, the value of LWE^* corresponding with the difference in void fraction of 0.45 is proposed to differentiate the slug flow and the churn flow. When the gas flow reaches certain values, the chaotic nature characteristic make the CCF inapplicable; hence, the *LDR* value can not be estimated. In these cases, the *MVF* is used again (larger than 0.4) with the LWE^* coefficient for characterizing churn flow.

The estimated uncertainty of each flow condition is shown in Fig. 12. At low gas flow rate, the small uncertainty indicates the stable development of cap bubbly flow regime. As the gas flow is increased, the bubbly-to-slug transition occurs and the uncertainty is gradually increased which shows the unsteady characteristic of transition. Large uncertainty in churn flow shows very clearly the chaotic nature of slug-to-churn and churn flow.

In summary, the criteria for differentiating the discrete bubbly flow, the cap bubbly flow, the slug flow, and churn flow can be described as follows:

- Discrete bubbly flow: $LWE^* < 10^{-4}$, $MVF < 0.2$.
- Cap bubbly flow: $10^{-4} < LWE^*$, $LDR < 2$.
- Slug flow: $LWE^* > 0.04$, $LDR > 2$.
- Churn flow: $LWE^* < 0.04$, $LDR > 2$ or $MVF > 0.4$.

Based on these criteria, a concrete flow chart of discrimination method has been proposed in Fig. 13. First, the time record of void fraction for 10 s is processed to produce the *MVF* value and the LWE coefficients map. The local peaks information is obtained by the software developed in MATLAB® in order to estimate the LWE^* coefficient and the effective scale. The effective scale is combined with the propagation speed to estimate the *LDR* value. Then three objective indicators are used to classify the flow patterns based on the criteria proposed above. Fig. 14 shows the comparison between the performance of the present method and Taitel et al.'s (1980) flow regime map. As can be seen, the transition from bubbly to slug

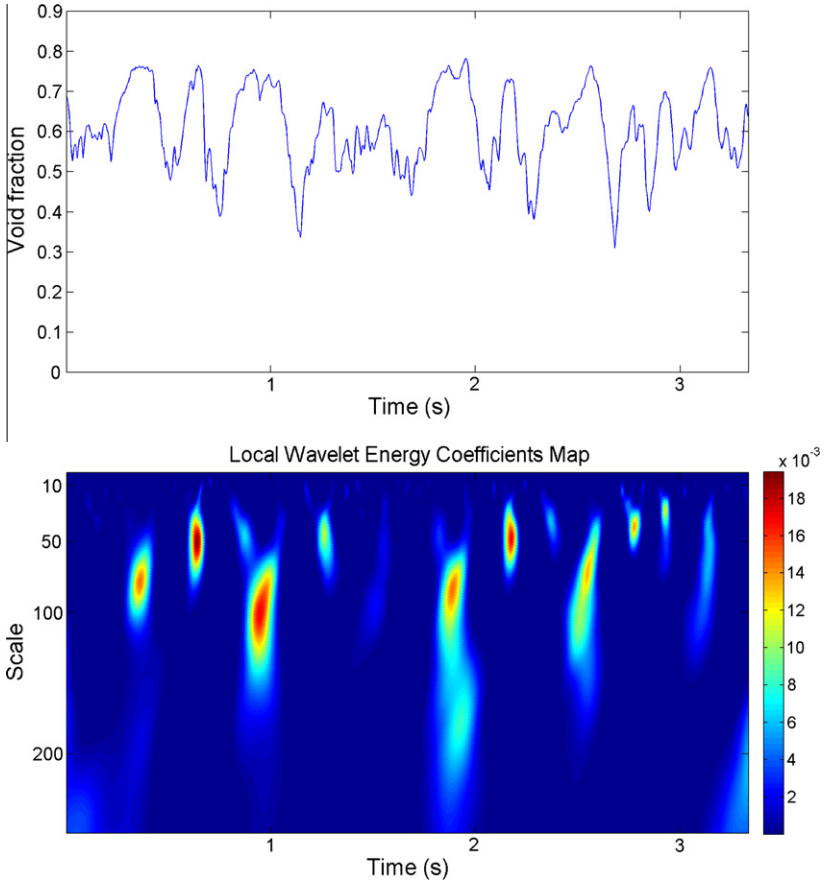

Fig. 10. Typical signal of churn/turbulent flow.

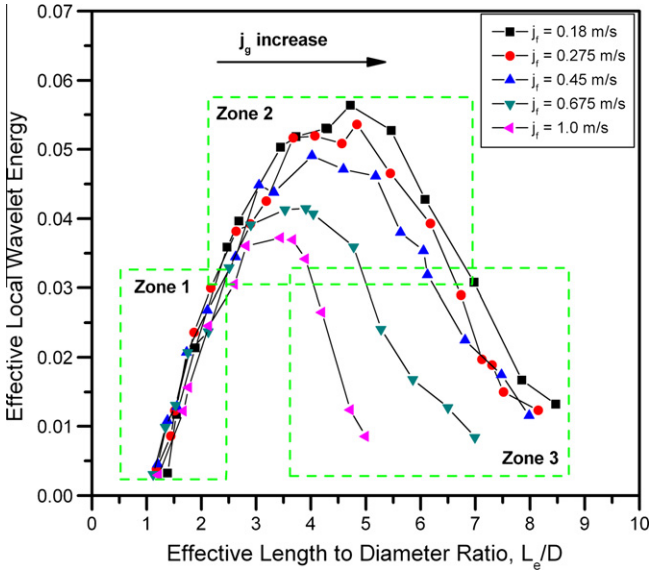

Fig. 11. Flow patterns identification map.

flow is indicated almost at the same flow rates in both the cases. Moreover, the entry length effect of churn flow proposed by Taitel et al. (1980) is clearly shown to confirm the accuracy of this discrimination method.

6. Conclusions

In this paper, an application of the wavelet analysis technique for two-phase flow pattern identification in vertical air–water flow has been investigated. The fluctuations of void fraction, which can reveal the characteristics of the structures of the discrete phase in two-phase flow, were measured from a multi-channel Impedance Void Meter (IVM), and then were analyzed by the Wavelet analysis technique. It has been shown that the Continuous Wavelet Transform (CWT) using Daubechies' mother wavelet is applicable in the objective discrimination of two-phase flow patterns using void fraction signals.

The local wavelet energy (LWE) coefficients map obtained from CWT provides a joint time-and-frequency analysis of void fluctuations, then it is possible to characterize both the periodic and intermittent flows. From this map, the effective LWE coefficient and the effective length-to-diameter ratio (LDR) were developed and they have been proved to be used as objective indicators for two-phase flow patterns identification based on an extensive experimental data. Its comparison with Taitel et al.'s analytical flow regime map shows that the proposed method has high precision for characterizing different flow regimes, and this method hold considerable promise for online recognition of two-phase flow patterns due to the short time processing.

However, further studies, such as the accurate correlation between the ratio of bubbles length-to-diameter and the effective length-to-diameter ratio, as well as the improvement of the flow patterns identification method are still required.

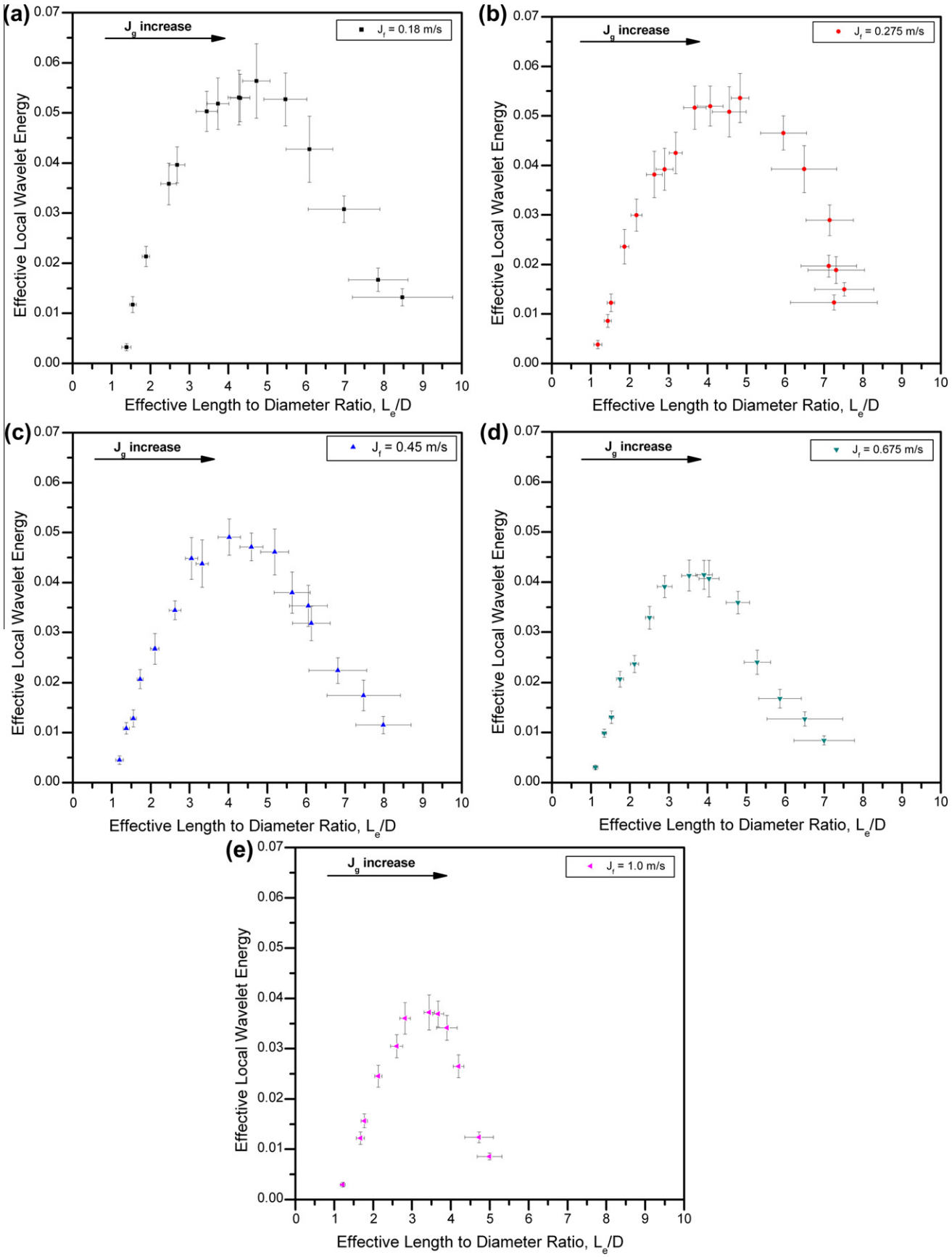

Fig. 12. Uncertainty of 100 consecutive tests at each flow condition: (a) $J_f = 0.18$ m/s, (b) $J_f = 0.275$ m/s, (c) $J_f = 0.45$ m/s, (d) $J_f = 0.675$ m/s, and (e) $J_f = 1.0$ m/s,

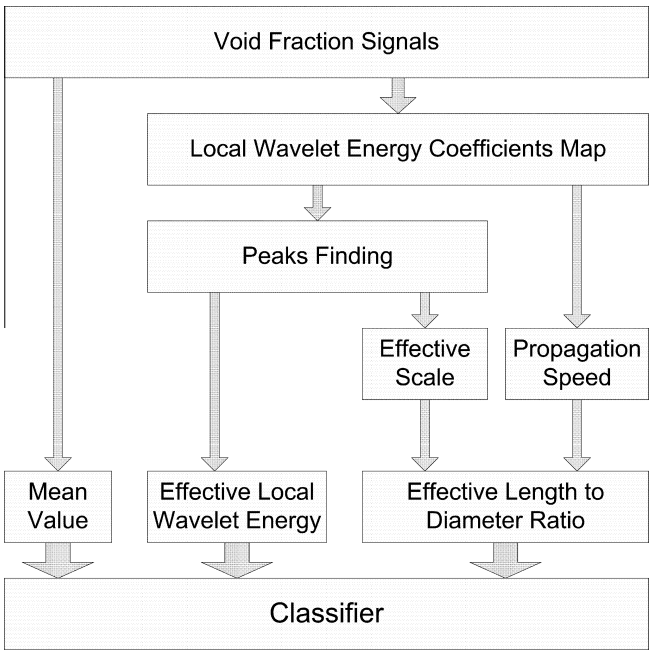

Fig. 13. Flow chart of identification method.

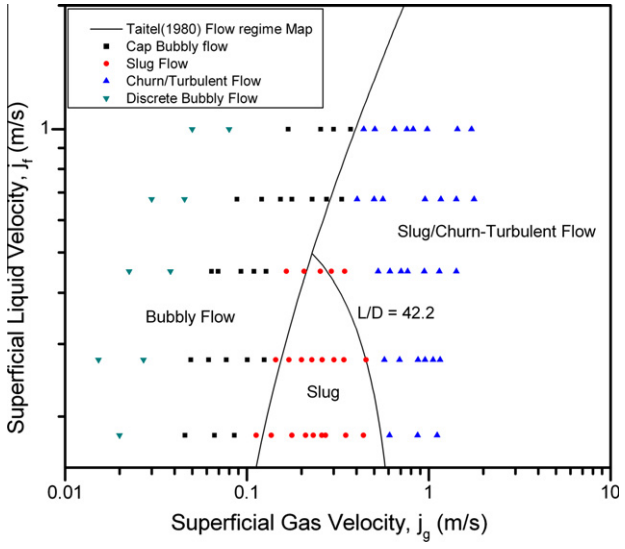

Fig. 14. Performance of identification method.

Acknowledgement

This work was supported by the Nuclear Research and Development Program of the National Research Foundation (NRF) Grant funded by the Korean Government (MEST) (Grant code: M20702040003-08M0204-00310).

Appendix A. Supplementary material

Supplementary data associated with this article can be found, in the online version, at doi:10.1016/j.ijmultiphaseflow.2010.04.007.

References

Barnea, D., Shoham, O., Taitel, Y., 1980. Flow pattern characterization in two phase flow by electrical conductance probe. Int. J. Multiphase Flow 6, 387–397.

Costigan, G., Whalley, P.B., 1997. Slug flow regime identification from dynamic void fraction measurements in vertical air–water flows. Int. J. Multiphase Flow 23, 263–282.

Daubechies, I., 1992. Ten Lectures on Wavelets. CBMS-NSF Regional Conference Series in Applied Mathematics, Society of Industrial and Applied Mathematics 61, Philadelphia.

Delhaye, J.M, Favreau, C., Saiz-Jabardo, J.M, Tournaire, A., 1987. Experimental investigation on the performance of impedance sensors of two and six electrodes for area averaged void fraction measurements. In: Proc. 24th National Heat Transfer Conf., Pittsburgh, PA, pp. 234–239.

Duckler, A.E., Taitel, Y., 1986. Flow pattern transition in gas-liquid systems: measurement and modeling. In: Hewit, G.F., Delhaye, J.M., Zuber, N. (Eds.), Multiphase Science and Technology, vol. 2. Hemisphere, Washington, DC, pp. 1–94.

Elperin, T., Klochko, M., 2002. Flow regime identification in a two-phase flow using wavelet transform. Exp. Fluids 32, 674–682.

Euh, D.J., 2002. A Study on the Measurement Method and Mechanistic Prediction Model for the Interfacial Area Concentration. Ph. D. Thesis, Seoul National Univ., Seoul, Korea.

Fagundes Netto, J.R., Fabre, J., Pereson, L., 1999. Shape of long bubbles in horizontal flow. Int. J. Multiphase Flow 25, 1129–1160.

Farge, M., 1992. Wavelet transforms and their applications to turbulence. Annu. Rev. Fluid Mech. 24, 395–457.

Hewiit, G.F., Jayanti, S., 1993. To churn or not to churn. Int. J. Multiphase Flow 19, 527–529.

Hewitt, G.F., Hall Taylor, N.S., 1970. Annular Two Phase Flow. Pergamon Press.

Hubbard, M.G., Dukler, A.E., 1966. The characterization of flow regimes for horizontal two-phase flow. In: Saad, M.A., Moller, J.A. (Eds.), Proc. 1966 Heat Transfer and Fluid Mechanics Institute, Stanford University Press, pp. 100–121.

Jayanti, S., Hewitt, G.F., 1992. Prediction of the slug-to-churn flow transition in vertical two-phase flow. Int. J. Multiphase Flow 18, 847–860.

Jones Jr., O.C., Zuber, N., 1975. The interrelation between void fraction fluctuations and flow patterns in two-phase flow. Int. J. Multiphase Flow 2, 273–306.

Kirpalani, D.M., Sparks, B.D., McCracken, T.W., 2001. A wavelet based approach for determining two-phase flow patterns. In: Michelides, E.E. (Ed.), Proc. 4th International Conference on Multiphase Flow, New Orleans. Tulane University, New Orleans.

Kulkarnia, A.A., Joshia, J.B., Kumarb, V.R., Kulkarnib, B.D., 2001. Application of multiresolution analysis for simultaneous measurement of gas and liquid velocities and fractional gas hold-up in bubble column using LDA. Chem. Eng. Sci. 56, 5037–5048.

Letzel, H.M., Schouten, J.C., Krishna, R., Van den Bleek, C.M., 1997. Characterization of regimes and regime transitions in bubble columns by chaos analysis of pressure signals. Chem. Eng. Sci. 52, 4447.

Li, T., Li, Q., Zhu, S., Ogihara, M., 2002. A survey on wavelet applications in data mining. ACM SIGKDD Explor. Newsl. 4, 49–68.

Lin, T.-J., Juang, R.-C., Chen, Y.-C., Chen, C.-C., 2001. Predictions of flow transitions in a bubble column by chaotic time series analysis of pressure fluctuation signals. Chem. Eng. Sci. 56, 1057.

Mao, Z.S., Dukler, A.E., 1993. The myth of churn flow? Int. J. Multiphase Flow 19, 377–383.

Matsui, G., 1986. Automatic identification of flow regimes in vertical two-phase flow using differential pressure fluctuations. Nucl. Eng. Des. 95, 221–231.

Mishima, K., Ishii, M., 1984. Flow regime transition criteria for upward two-phase flow in vertical tubes. Int. J. Heat Mass Transfer 27, 723–737.

Nedeltchev, S., Shaikh, A., Al-Dahhan, M., 2006. Flow regime identification in a bubble column based on both statistical and chaotic parameters applied to computed tomography data. Chem. Eng. Technol. 29, 1054.

Nedeltchev, S., Jordan, U., Lorenz, O., Schumpe, A., 2007. Identification of various transition velocities in a bubble column based on Kolmogorov entropy. Chem. Eng. Technol. 30, 534.

Seleghim Jr., P., Milioli, F.E., 2001. Improving the determination of bubble size histograms by wavelet de-noising techniques. Powder Technol. 115, 114–123.

Shang, Z., Yang, R., Cao, X., Yang, Y., 2004. An investigation of two-phase flow instability using wavelet signals extraction technique. Nucl. Eng. Des. 232, 157–163.

Song, C.-H., No, H.C., Chung, M.K., 1995. Investigation of bubble flow developments and its transition based on the instability of void fraction waves. Int. J. Multiphase Flow 21, 381–404.

Song, C.-H., Chung, M.K., No, H.C., 1998. Measurements of void fraction by an improved multichannel conductance void meter. Nucl. Eng. Des. 184, 269–285.

Song, C.-H., Baek, W.P., Park, J.K., 2007. Thermal-hydraulic tests and analyses for the APR1400's development and licensing. Nucl. Eng. Technol. 39, 299–312.

Taitel, Y., Barnea, D., Dukler, A.E., 1980. Modelling flow pattern transitions steady upward gas–liquid flow in vertical tube. AIChE J. 26, 345–354.

Tournaire, A., 1986. Dependence of the instantaneous response of impedance probes on the local distribution of the void fraction in a pipe. Int. J. Multiphase Flow 12, 1019–1024.

Tutu, N.K., 1982. Pressure fluctuations and flow pattern recognition in vertical two phase gas–liquid flows. Int. J. Multiphase Flow 8, 443–447.

Van den Bleek, C.M., Schouten, J.C., 1993. Deterministic chaos: a new tool in fluidized bed design and operation. Chem. Eng. J. 53, 75.

Vince, M.A., Lahey, R.T., 1982. On the development of an objective flow regime indicator. Int. J. Multiphase Flow 8, 93–124.

Wallis, G.B., 1969. One-Dimensional Two-phase Flow. Mc-Graw-Hill Book Company, New York.

Wu, H.J., Zhou, F.D., Wu, Y.Y., 2001. Intelligent identification system of flow regime of oil–gas–water multiphase flow. Int. J. Multiphase Flow 27, 459–475.